愛媛大学農学部紀要 60 号：15－24（2015）
Memoirs of Faculty of Agriculture, Ehime University, 60: 15－24 (2015)

Measurement of Nitrogen Dioxide by Passive Samplers and Numerical Prediction by a Gaussian Plume-Puff Model in a Roadside Area of Mexico City

Isao KANDA*, Naohide SHINOHARA**, Felipe ÁNGELES GARCÍA***, and Shinji WAKAMATSU****

Abstract

To evaluate the air quality in the vicinity of a heavily trafficked road in the central part of Mexico City, the concentration of NO_2 was measured using passive samplers installed at various distances up to 150 m from the road. The measurement was conducted once for 24 hours in November 2011 in Plaza Vizcainas beside Eje Central. The obtained concentrations were about 50 ppbv and 30 ppbv at 2-m and 150-m from the curb, respectively, and both values were comparable to those reported in similar environments. For the condition during the sampling period, a Gaussian plume-puff model was employed to simulate the concentration of NO_2. Emission rate of nitrogen oxides was estimated based on a traffic census in 2003, a national emissions inventory, and on-site traffic counting. The model prediction was comparable to the measured values although the decay by distance from the road was much more gradual than the measurement.

Keywords: Air pollution, Mexico, Nitrogen dioxide, Passive sampler, Roadside

1. Introduction

Road traffic is a major source of air pollutants such as NO_2, BC, CO, and VOC that are associated directly or indirectly with adverse health effects (Heath Effects Institute, 2009). Transport and diffusion of the primary and secondary pollutants from roads are of great concern to people living or working in roadside areas. Concerns over roadside air pollution have increased as the overall air quality improved, the contrast between near-road and far-road regions intensified, and the people's desire for cleaner air became stronger.

In developed countries, considerable research on roadside air pollution has been conducted in the past (Roorda-Knape et al., 1998; Hitchins et al., 2000; Minakawa et al., 2000a,b; Kodama et al., 2002; Tiitta et al., 2002; Zhu et al., 2002; Naser et al., 2009). These previous studies were in large part motivated by lawsuits filed against the national governments and the related industries. In Japan, for example, the trials resulted in reconciliations that mandated the government to implement mitigation measures against air pollution. As described in Wakamatsu et al. (2013), the roadside air quality in Japan has improved considerably due to various stringent measures.

In developing countries, however, the roadside air pollution is not well understood. On one hand, there is a better awareness to air quality due to the enhanced information exchange across the globe through the internet. On the other hand, there are few air-monitoring stations in the immediate neighborhood of major roads. Therefore, even if people living in the roadside areas suffer from health problems and suspect the influence of the road traffic, there are no quantitative information on

Received 1 April 2015
Accepted 31 July 2015
*Ehime University, Faculty of Agriculture, Department of Life Environmental Conservation
**National Institute of Advanced Industrial Science and Technology
***National Institute of Ecology and Climate Change, Mexico
****Ehime University, Faculty of Agriculture, Department of Life Environmental Conservation (Corresponding Author)

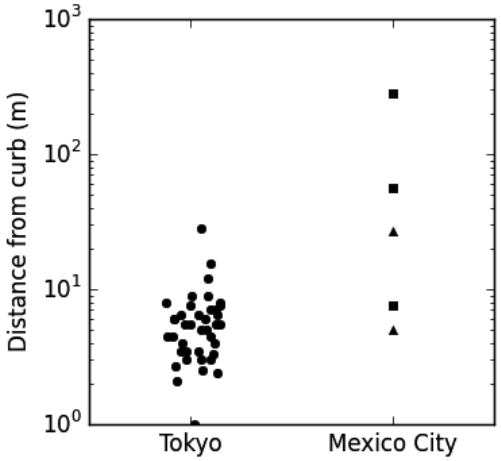

Fig. 1. Distance of roadside air-monitoring stations from curbs in Tokyo and Mexico City (square: traffic stations, triangles: industrial stations). The horizontal scatter of markers for Tokyo is random.

air quality that could be related to the health problems. Fig. 1 compares the curb distances of air-monitoring stations (as of year 2010) that are classified as 'roadside' in Tokyo and 'traffic' or 'industrial' in Mexico City. We observe that, in Tokyo, many (37) roadside stations existed within 10 m of major roads, but in Mexico City, only two stations were located within 10 m (one was in an industrial area, and did not represent a residential environment). Even if we account for the fact that the worst air pollution occurred nearly 20 years later in Mexico City (around 1990) than in Tokyo (around 1970), the number of stations within 10 m of major roads in Tokyo was already 23 in 1990.

In the absence of permanent air-monitoring stations, use of passive samplers is a feasible alternative for grasping the state of atmospheric environment (van Roosbroeck et al., 2006; Huang et al., 2013; Lee et al., 2014). Although accuracy and temporal resolution are inferior to automatic equipment used in permanent stations, passive samplers are inexpensive and can be installed easily at high spatial density. Numerical prediction models are also available, but they are subject to errors in input data such as vehicle emission and weather condition. In practice, numerical models must be applied in combination with on-site measurements by passive samplers or other methods to assure their accuracy.

In this article, we report a passive sampling experiment in a roadside area of downtown Mexico City. The experiment was intended to reveal the spatial variation of NO_2 concentration in the immediate vicinity of a major road. To assess the feasibility of numerical simulation models, the measurement result was compared with the prediction of a Gaussian diffusion model.

2. Method

2.1 Sampling site

The sampling was conducted in Plaza Vizcainas (99°08'27" W, 19°25'39" N; Fig. 2) beside Eje Central in the central area (Cuauhtémoc) of Mexico City, located on a high plateau about 2250 m from the mean sea level.

Fig. 2. Sampling points in Plaza Vizcainas, Mexico City (aerial photo from Google Earth).

Table 1. Sampling locations, periods, and results

No	Distance from curb (m)	Height from ground (m)	Height from road (m)	Begin Nov 24	End Nov 25	NO_2 (ppbv)
1	2	2.00	2.00	7.05	7.04	51.5
2	2	2.00	2.00	7.09	7.05	53.8
3	16	0.45	0.95	7.12	7.05	45.2
4	16	0.40	0.90	7.15	7.06	42.6
5	30	0.45	0.95	7.20	7.07	32.7
6	50	0.65	1.15	7.24	7.07	32.0
7	75	1.30	1.80	7.27	7.09	31.0
8	98	1.00	1.50	7.32	Lost	
9	150	0.50	1.00	7.37	7.10	32.0

Eje Central is a 6-lane road with the outer 2 lanes allocated to trolley buses that run by electricity, and the inner 4 lanes to other vehicles that run one-way toward north. The vehicle traffic volume is about 6×10^4 per day, consisting mostly of passenger cars. As a commercial and tourist center, there are many pedestrians on the sidewalks.

Plaza Vizcainas is a park with many trees about 10 m high. The park dimension is about 160 m by 25 m with the shorter side parallel to Eje Central. Beneath the park, there is an underground parking lot about the same horizontal extent as the park. The parking lot has a one-way structure with the entrance facing Eje Central and the exit on the opposite side. The entrance ramp down to the parking lot begins at about 15 m from the curb of Eje Central. Compared to the traffic flow on Eje Central, the number of cars entering the parking lot is negligibly small. Also, because the entrance is a down-slope, the emission from entering cars is less than that from cars running on Eje Central.

2.2 Sampling method

We used DSD-TEA passive samplers for acid gases (Sigma-Aldrich Co. LLC.). While the samplers are exposed to the ambient air, acid gases diffuse through the outer diffusion filter made of porous sintered polyethylene, and become adsorbed to the silica gel impregnated with triethanolamine (TEA).

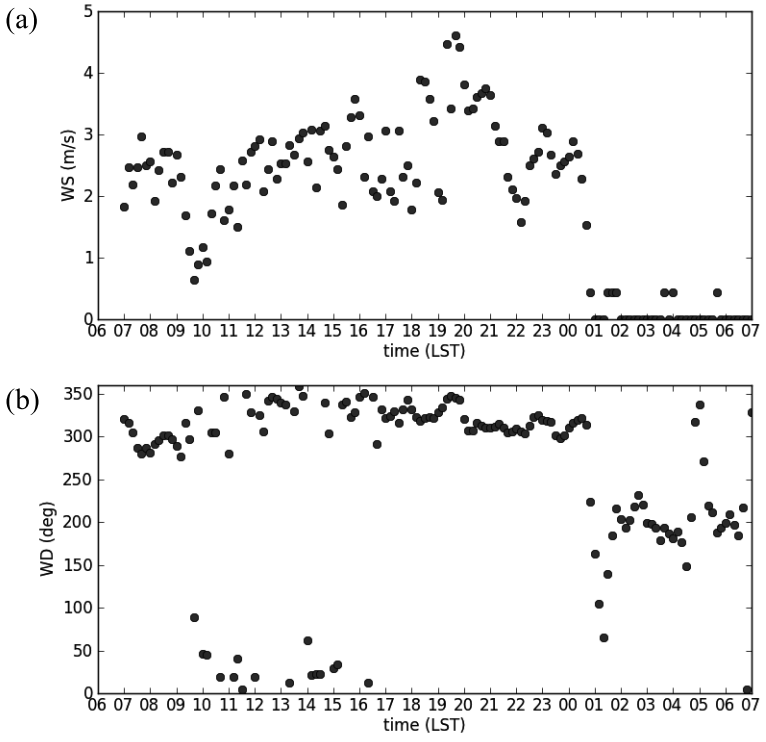

Fig. 3. Wind speed (a) and direction (b) during the sampling period.

The passive samplers were hung on tree branches from the morning of 24 November 2011 to the next morning. The locations and the sampling times are shown in Fig. 2 and Table 1. The distance from the curb of Eje Central was measured by a laser optical distance meter. At 2 m and 16 m distance from the curb, two points were set for each. The sampler at 75 m from the curb was found dropped in the evening of 24 November and was soon returned to the original position. The sampler at 98 m from the curb was found stolen in the morning of 25 November although it was intact in the evening of 24 November.

2.3 Weather condition

The meteorological condition during the sampling period was obtained from Sevicio Meteorológico Nacional (SMN) located 6.4 km to west-south-west from the sampling site. This distance can be regarded small compared to the size of the Mexico City basin (40 km west-to-east and 60 km south-to-north).

There was no rainfall during the sampling period. The mean temperature and pressure were 15.8 °C and 777 hPa, respectively. Fig. 3 shows the wind speed and direction. In the daytime, the wind was from around the north and the wind speed was moderate (2-4 m s^{-1}). From 1 to 7 o'clock, the wind was calm and was often below the detection limit 0.4 m s^{-1}. The vertical profiles of the temperature measured at SMN by radiosonde at 6 and 18 o'clock showed no sign of surface temperature inversion that could affect the dispersion behavior of pollutants considerably.

2.4 Sample analysis

The adsorbed acid ions were eluted out with 5 ml HPLC-grade ultra-pure water on 25 November, and were stored in a refrigerator. A blank sample that was not exposed to the ambient air was also eluted out. The eluted solution was put to ion chromatography analysis on 1 December 2011 and 25-27 January 2012. In this article, we consider only NO_2^- that derives from gaseous NO_2.

The ion mass W (g) that diffused through the sampler filter is given by

$$W = W_s - W_b \tag{1}$$

where W_s and W_b are the mass of the ion in the exposed sampler and the blank, respectively. If we write the rate of flux of the concerned acid gas (A) through the diffusion filter as J (mol s^{-1}), we find

$$Jt = \frac{W}{M}, \tag{2}$$

where M is the molecular mass of A, and t (s) is the sampling duration. It is convenient to write J in terms of the sampling flow rate R ($m^3 s^{-1}$) defined by

$$J = Rn, \tag{3}$$

where n (mol m^{-3}) is the molar concentration of A in the atmosphere. If the diffusion filter of the sampler is a uniform plate with thickness L (m) and area S (m^2), we find

$$R = \frac{D}{L}S, \tag{4}$$

where D ($m^2 s^{-1}$) is the diffusion coefficient. We note that the typical pore size of the diffusion filter is at least 1 μm, much larger than the mean free path ~68 nm of air molecules in the standard atmosphere. Hence, the transport through the filter is in the continuum regime where inter-molecule collisions are the major impedance rather than in the Knudsen diffusion regime where molecule-wall collisions make major drag.

Fuller et al. (1966), summarizing numerous experimental results, deduced the following relation for the binary diffusion of gas species A and B,

$$D_{AB} \propto \frac{T^{1.75}}{P} f_{AB}, \tag{5}$$

where

$$f_{AB} = \frac{\left(1/M_A + 1/M_B\right)^{1/2}}{\left(\sum_i v_{A,i}\right)^{1/3} + \left(\sum_i v_{B,i}\right)^{1/3}}, \tag{6}$$

P (hPa) is the pressure, T (K) is the absolute temperature, M_A and M_B are molecular masses of A and B, respectively, and $v_{A,i}$ and $v_{B,i}$ are the diffusion parameters related to atoms, groups, and structural features.

By comparison with active-pumping sampling, Uchiyama et al. (2004) found

$$R_{HCHO}^{1\ atm,\ 25\ ^\circ C} = 71.9\ mL\ min^{-1} \tag{7}$$

for formaldehyde (HCHO) diffusing in air at P=1013 hPa (1 atm) and T=298.15K (25°C) for passive samplers with the same diffusion filter as that used in our measurement. Substituting (5) and (6) into (4), the sampling flow rate $R_A^{P,T}$ for species A at pressure P and temperature T becomes

$$R_{\mathrm{A}}^{P,T} = R_{\mathrm{HCHO}}^{1\ \mathrm{atm},\ 25\ ^{\circ}\mathrm{C}} \frac{1013}{P}\left(\frac{T}{298.15}\right)^{1.75} \frac{f_{\mathrm{A,air}}}{f_{\mathrm{HCHO,air}}} . \quad (8)$$

Here, we comment on Graham's law of gas diffusion through porous media. Graham's law states that the diffusion flux in a binary mixture through porous media is inversely proportional to the square root of molecular weight, i.e.,

$$\frac{J_{\mathrm{A}}}{J_{\mathrm{B}}} = \sqrt{\frac{M_{\mathrm{B}}}{M_{\mathrm{A}}}} . \quad (9)$$

Graham's law was established in a closed system in the gas phase where the pressure on both sides of the porous media was maintained equal, which led to non-zero net flux $J_{\mathrm{A}} + J_{\mathrm{B}}$ that was not described by Fick's law (3) and (4). This condition is not met in the passive sampler where the acid gas diffusing through the porous filter is immediately adsorbed by the TEA-soaked silica gel. A detailed description of the nature of Graham's law can be found in Mason and Malinauskas (1983).

Substituting (8) into (2) and (3), and using the relation between volume mixing ratio C_{A} (ppbv) and molar concentration n

$$C_{\mathrm{A}} = 22.4\times10^{-3}\frac{1013}{P}\frac{T}{273.15}n\times10^{9}, \quad (10)$$

we obtain

$$C_{\mathrm{A}} = 22.4\times10^{-3}\frac{W\times10^{9}}{M_{\mathrm{A}}t\left(\frac{T}{298.15}\right)^{0.75}R_{\mathrm{HCHO}}^{1\ \mathrm{atm},\ 25\ ^{\circ}\mathrm{C}}}\frac{f_{\mathrm{HCHO,air}}}{f_{\mathrm{A,air}}} \quad (11)$$

Despite the previous argument on Graham's law, Uchiyama et al. (2004) assumed

$$\frac{f_{\mathrm{HCHO,air}}}{f_{\mathrm{A,air}}} = \sqrt{\frac{M_{\mathrm{A}}}{M_{\mathrm{HCHO}}}} . \quad (12)$$

That this relation is inappropriate can be shown by plotting experimental values of diffusivity for binary gas mixtures. Fig. 4 shows diffusivity $D_{\mathrm{A,N_2}}$ of various molecules A mixed with nitrogen at pressure 1013 hPa and temperature 298.15 K calculated by the empirical relations in Marrero and Mason (1972). We observe that no simple linear relationship exists between $1/\sqrt{M_{\mathrm{A}}}$

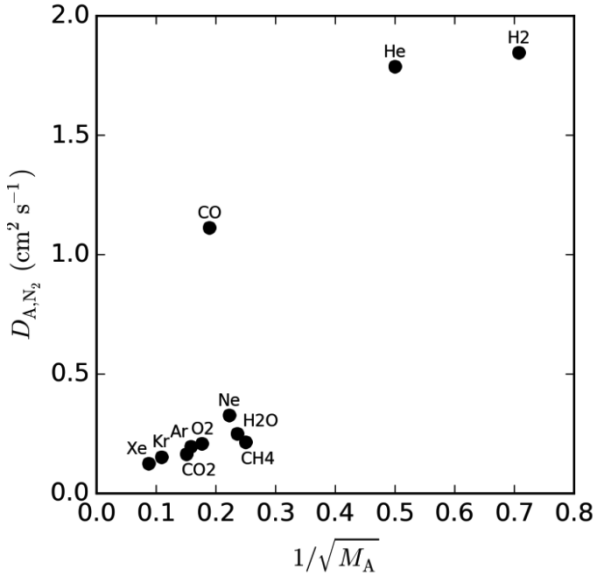

Fig. 4. Relationship between molecular mass M_{A} and diffusivity $D_{\mathrm{A,N_2}}$ in a binary mixture of A and N_2 at 1013 hPa and 298.15 K. The values of $D_{\mathrm{A,N_2}}$ were calculated using the empirical relations reported in Marrero and Mason (1972).

and $D_{\mathrm{A,N_2}}$. However, because calculation of the factor (6) for HCHO-air or NO_2-air combination could not be conducted readily, we tentatively adopted (12) with A=NO_2, P=777 hPa, and T=288.95K (15.8 °C) in the following analysis.

3. Measurement result

The measurement results of $C_{\mathrm{NO_2}}$ are listed in the right-most column in Table 1. We observe that $C_{\mathrm{NO_2}}$ decayed by the distance from the curb and became nearly constant at 30 m. At the 2-m points, the contribution from the road was about 2/3 of the background value. The two points each at 2 m and 16 m from the curb had similar values, indicating that there was not substantial spatial variation of the concentration field parallel to the road.

We examine the plausibility of the measurement on two aspects: background concentration and contribution from the road-traffic emission. With respect to the background concentration, we compare the 150 m-point value and those measured at neighboring monitoring stations. Near the sampling site, there were 4 stations where concentrations of NO and NO_2 were measured by automatic equipment during our sampling period. At three of these stations, the concentration ratio NO/NO_2 was found to have large peaks in the morning rush hour, indicating considerable effects of road-traffic emissions. In contrast, at one station (Pedregal) located on the roof-top of a two-story primary school in a residential

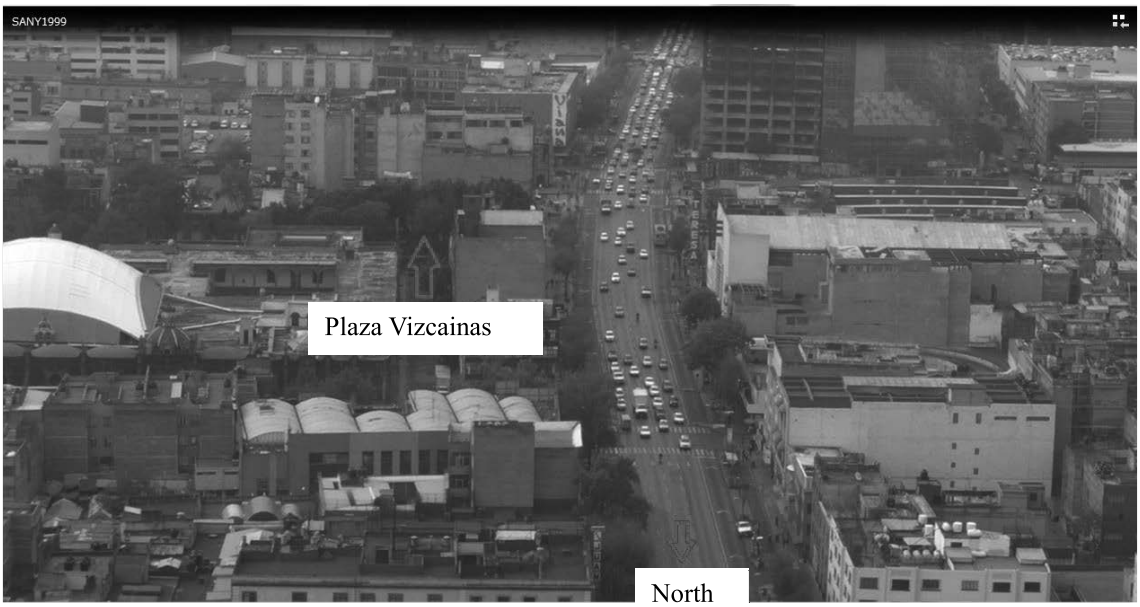

Fig. 5. A sample still capture image of the video recording from Latin American Tower

area, the morning peak of NO/NO_2 was much smaller. Therefore, we may assume that the concentration of NO_2 at the Pedregal station was representative of the background state. The mean concentration of NO_2 at the Pedregal station during our sampling period was 26.6 ppbv, which is close to our 150 m-point value 32.0 ppbv.

We next examine if the measured concentration at the 2-m points was realistic. Because it is the absence of roadside stations that motivated our study, there was no appropriate reference station in Mexico City. Instead, we consider Japanese stations (Miyagawashougakkou, Dekijimashougakkou, Motoshikoen, Kamiuma, and Hachimanyama) that are in urban areas and are close to the curbs of heavily trafficked roads. An appropriate background station was selected for each of these roadside stations. On weekdays from 12 to 16 March 2009, nondescript spring days, the average concentration differences of NO_2 between roadside and background stations were 30.1, 9.5, 11.5, 25.6, and 18.0 ppbv, respectively in the above mentioned order. Therefore, the measured road-traffic contribution (about 20 ppbv) at the 2-m stations can be regarded realistic.

4. Model simulation

4.1 Estimation of emission rate

4.1.1 Traffic counting

The traffic flow on Eje Central was monitored from the visitors' deck of the Latin American Tower (183 m) about 710 m to the north of Plaza Vizcainas. The traffic flow was recorded on a video camera three times in the morning of 24 November 2011 after installing the samplers. A still capture image is shown in Fig. 5. The recording was limited to only three times due to security concerns as advised by Mexican research organizations. The beginning time and the duration of the recordings are listed in Table 2. The traffic volume was measured by a tally counter while playing back the video recordings. The vehicles were categorized into passenger cars, small trucks, normal trucks, and buses. Only one normal truck passed during the recording time. The results are listed in Table 2 where the normal trucks and buses are combined.

An extensive traffic monitoring campaign was conducted in 2003 by the government of Mexico City (Distorito Federal). On Eje Central, the monitoring point closest to our sampling site was about 1.3 km to the north of Plaza Vizcainas. The monitoring was done for a week with Trax I Plus (JAMAR Technologies Inc.) that made use of the pressure pulse when car tires stepped on elastic tubes laid across the road. Fig. 6 shows the mean hourly flows of passenger cars and trucks (of all sizes) on weekdays. We observe that the flow rate in 2003 was about twice as small as during our measurement. Another important difference is the substantially higher ratio of large trucks in 2003; the ratio of small and large trucks combined were about 8 % in both the 2003 census and our measurement, but the ratio of large trucks with 4 or more axles was 7 % in 2003, occupying most of the trucks.

Table 2. Video recording time and results on 24 November 2011. Numbers in parenthesis indicate equivalent counts in an hour.

Start time (LST)	Duration (min)	Passenger cars	Small trucks	Normal Trucks/Buses
9:21:04	8	400 (3000)	12 (90)	3 (22.5)
10:21:30	6	229 (2290)	28 (280)	2 (20)
11:22:14	6	248 (2480)	30 (300)	1 (10)

Therefore, the diurnal pattern in the 2003 census needed to be adjusted for the traffic volume and the ratio of large trucks. The volume adjustment ratio α was defined as the mean hourly traffic flow rate of passenger cars or small trucks during our traffic counting period divided by the mean hourly traffic flow rate of passenger cars from 9:00 to 11:00 in the 2003 census. We obtained $\alpha_{\text{passenger cars}}=2.27$ and $\alpha_{\text{small trucks}}=0.196$ for small trucks. For normal trucks and buses, we assumed that only buses run on Eje Central in the day time (6:00 - 24:00) with ratio β of (normal trucks + buses) to (passenger cars + small trucks) being 0.0062, derived using the values in Table 2, and no heavy-duty vehicles run at night (β=0). In summary, the estimated vehicle flow rate V (type,h) became,

$$V(\text{passenger cars},h)=\alpha_{\text{passenger cars}}V_{\text{DF2003}}(\text{passenger cars},h) \quad (13)$$

$$V(\text{small trucks},h)=\alpha_{\text{small trucks}}V_{\text{DF2003}}(\text{small trucks},h) \quad (14)$$

$$V(\text{buses},h)=\begin{cases}\beta\left(V(\text{passenger cars},h)+V(\text{small trucks},h)\right) & (6\le h\le 24)\\ 0 & (\text{otherwise})\end{cases} \quad (15)$$

where V_{DF2003}(passenger cars,h) is the diurnal pattern of traffic flow rate in the 2003 census shown by circles in Fig. 6.

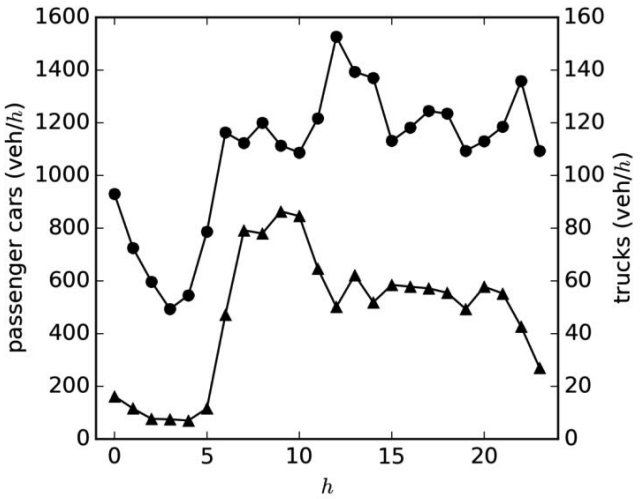

Fig. 6. Diurnal patterns of traffic volume. Circles: V_{DF2003} (passenger cars, h), triangles: V_{DF2003} (trucks, h).

4.1.2 Emission rate

Emission rate Q (h) of NOx (=NO+NO_2) can be obtained as the sum of products between emission factor ε and traffic flow rate V of all the relevant types of vehicles. Emission factor ε of exhaust pollutants is usually prepared for different vehicle types, model years, and fuel types. In Mexico, such categorized values of ε is often generated by the MOBILE software (US-EPA, 2015). For a base year 2008, we obtained, through an institutional agreement, categorized values of ε calculated using MOBILE v.6.2 (with modified emissions database for the Mexican vehicle fleet) by SEMARNAT (Secretaria de Medio Ambiente y Recursos Naturales) of Mexico. Taking average weighing by the number of vehicles in each category, weighted-average emission factors ε (g km^{-1} $vehicle^{-1}$) of NOx by LDV (light-duty passenger vehicles), LDT (light-duty trucks), and HDV (heavy-duty vehicles) in Cuauhtémoc were obtained as

$$\varepsilon_{\text{LDV}}=1.52,\ \varepsilon_{\text{LDT}}=2.87,\ \varepsilon_{\text{HDV}}=20.78. \quad (16)$$

Note that the emission factor of NOx is defined in terms of the mass of NO_2 and that each vehicle category includes all fuel types (gasoline, diesel, liquid petroleum gas, and natural gas). These values are considerably higher than those in Japan; for the Kanto area in Japan, Naser et al. (2009) obtained 0.17 for passenger cars, 0.58 for small trucks, and 3.5 for normal trucks traveling at 20 km h^{-1}.

Vehicle exhaust emission is enhanced substantially when the vehicles are idling or starting from a stall. In front of Plaza Vizcainas, Eje Central does not cross with busy roads. The stop line at the crossing between Eje Central and another major road (Arcos de Belén - José Maria Izazaga) is about 130 m to the south. Hence, the effect of vehicle acceleration upon change of the traffic signal could be assumed negligible.

Finally, using the traffic volumes V(type,h) (vehicles h^{-1}) in (13-15), the emission rate Q(h) (g m^{-1} s^{-1}) from the road traffic becomes

$$Q(h) = \frac{1}{3600 \times 1000} \{ \varepsilon_{\mathrm{LDV}} V(\text{passenger cars}, h) + \varepsilon_{\mathrm{LDT}} V(\text{small trucks}, h) + \varepsilon_{\mathrm{HD}} V(\text{buses}, h) \}. \quad (17)$$

Fig. 7 shows the calculated results.

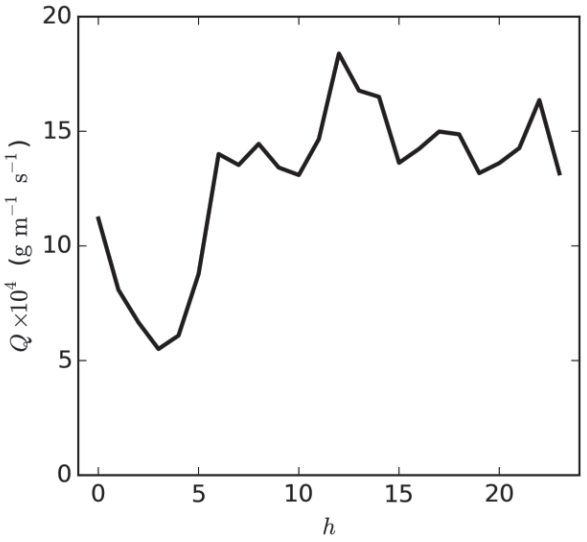

Fig. 7. Diurnal pattern of the estimated emission rate $Q(h)$.

4.2 Gaussian plume-puff model

Using the meteorological data and the estimated emission rate, we applied a numerical model to simulate the concentration field of NO_2. The model used was the Japanese plume-puff model, an empirical Gaussian diffusion model based on the guidelines of the Japan Ministry of Environment (Japan Environmental Agency, 2000). Salient features of the model are described below.

(i) Surface roughness: This model classifies surface roughness collectively as urban or rural, and hence does not reflect the effect of individual buildings. The roughness around the sampling site was classified as urban.

(ii) Time allocation of meteorological data: Following the Japanese convention, the hourly-averaged weather condition was represented by the 10-min average prior to the hour, i.e., the average from 1 a.m. to 2 a.m. was represented by the average from 1:50 to 2:00. The atmospheric stability for the hour was also determined using the 10-min average values.

(iii) Atmospheric stability: The width of the pollutant plume is defined as a function of atmospheric stability categorized into discreet classes (Pasquill-Gifford classes) depending on the wind speed,

Table 3. Concentrations (ppbv) of NO, NO_2, and O_3 measured by Minoura & Ito (2010) near a heavily trafficked road in Tokyo, Japan.

	0 m	20 m	100 m
NO	130.8	37.8	11.4
NO_2	50.2	30.9	20
O_3	15.7	20.7	23.5

and the radiation budget or cloud coverage. However, in Mexico City, the radiation budget or cloud coverage was available only in the daytime but not at night. Because surface thermal inversion was not observed in the mornings of 24 and 25 November 2011, we assumed that the nighttime stability was neutral (Pasquill-Gifford class D). In the daytime, the stability class ranged from A (unstable) to D.

(iv) Weak-wind treatment: Under weak-wind conditions (less than 1 m s^{-1}), the wind direction was considered indeterminate, and the concentration was calculated as the average of the results at 1 m s^{-1} for all the wind directions.

(v) Unit conversion: With the emission rate Q of NOx given in g s^{-1} m^{-1}, the resulting concentration $\hat{C}_{\mathrm{NOx}}^{\mathrm{mass}}$ is output in g m^{-3}. Conversion to the mixing ratio $\hat{C}_{\mathrm{NOx}}$ in ppbv was done by

$$\hat{C}_{\mathrm{NOx}} = \hat{C}_{\mathrm{NOx}}^{\mathrm{mass}} \frac{1}{M_{\mathrm{NO_2}}} \times 22.4 \times 10^{-3} \times \frac{1013}{777} \times \frac{288.95}{273.15} \times 10^9. \quad (18)$$

(vi) Species conversion: Nitrogen oxide is emitted from vehicles mostly (95 - 98 %) in the form of nitrogen monoxide NO, and is transformed into NO_2 by reaction with O_3. The timescale of this reaction is on the order of a minute, which multiplied by a typical wind speed (say, 3 m s^{-1}) leads to reaction lengthscale on the order of a few hundred meters. Because the spatial extent of our sampling is on the same order of this reaction lengthscale, the ratio NO_2 / NOx should vary substantially among the sampling points. Minoura & Ito (2010) reports measurements of NO, NO_2, and O_3 at various heights from the ground and at various distances from a heavily-trafficked road in Tokyo, Japan. Their results at 1 m from the ground are recapitulated in Table 3. Assuming that the concentrations at the 100-m point represent the general background condition, we find

$$\hat{C}_{\mathrm{NO_2}} = \hat{C}_{\mathrm{NOx}} (0.2 + 0.0045d). \quad (19)$$

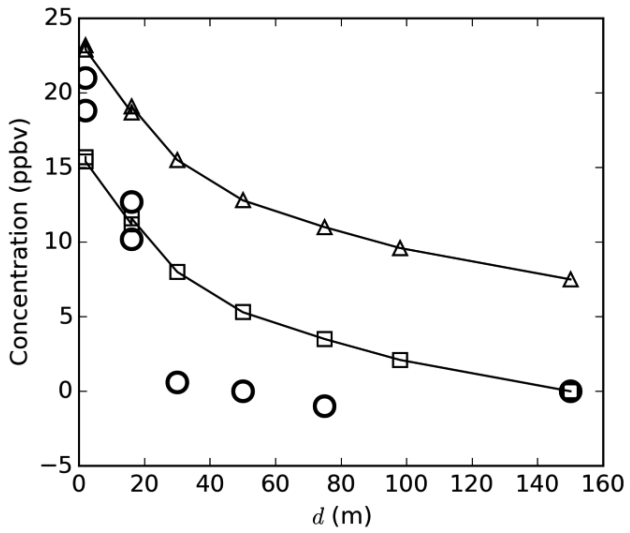

Fig. 8. Road-distance profiles of NO_2 concentration. Circles: field measurement C_{NO_2} - C_{NO_2} (d=150 m), triangles: model simulation $\hat{C}_{NO_2}$, squares: modified model simulation $\hat{C}_{NO_2}$ - $\hat{C}_{NO_2}$ (d=150 m).

The average concentration over the sampling period was calculated as the average of the 24 hourly predictions from 7 a.m. to the next-day 7 a.m. Fig. 8 compares the plume-puff model calculation with the field measurement. For the field measurement, the value at the 150-m point is subtracted as the background concentration. We observe that the model prediction (triangles) is about the same as the field measurement (circles) near the road. However, the decay with the distance from the road is more gradual in the model than in the measurement. The difference is clear even if we subtract the modeled 150-m value from the other modeled values (squares).

A possible cause of the difference in the decay behavior is the wind condition. As shown in Fig. 3, the wind direction was north in the daytime and south at night, and the wind speed was below the detection limit at night. The wind directions were therefore almost parallel to Eje Central during the sampling period. Road-parallel wind directions and low wind speed are known to cause large uncertainties in the plume-puff model predictions.

5. Summary

We conducted roadside passive sampling of ambient NO_2 in the central area of Mexico City, and compared the measured concentration with the prediction by a numerical model. The measured concentration was comparable to the levels observed elsewhere in similar environments. Despite the involved large uncertainties, the numerical simulation by a Gaussian plume-puff model produced concentration values fairly close to the field observation. Therefore, both the passive sampling and the Gaussian plume-puff model were found to be feasible methods for evaluating the air quality in the roadside environment in Mexico City. The methods established in this study will also be useful in deciding the locations of new roadside air-monitoring stations in Mexico City.

Acknowledgements

This work was conducted as part of "Joint Research Project on Formation Mechanism of Ozone, VOCs, and $PM_{2.5}$ and Proposal of Countermeasure Scenarios" funded by Japanese agencies JST and JICA under the SATREPS scheme. We are grateful to Mr. Hugo Landa Fonseca of SEMARNAT (Secretaria de Medio Ambiente y Recursos Naturales) of Mexico for providing the raw data of the mobile-source emissions that were used to construct Inventario Nacional de Emisiones de México 2008. We also appreciate Rolando Mendoza Ursulo for inspecting the installed samplers frequently.

References

Fuller, E.N., Schettler, P.D., and Giddings, J.C. (1966) A new method for prediction of binary gas-phase diffusion coefficients, Industrial and Engineering Chemistry 58: 19-27.

Health Effects Institute (2009) Traffic-related air pollution: A critical review of the literature on emissions, exposure, and health effects, Special Report 17, Health Effects Institute, U.S.A.

Hitchins, J., Morawska, L., Wolff, R., and Gilbert, D. (2000) Concentration of submicrometer particles from vehicle emissions near a major road, Atmospheric Environment 34: 51-59.

Huang, Y.K., Luvsan, M.E., Gombojav, E., Ochir, C., Bulgan, J., and Chan, C.C. (2013) Land use patterns and SO2 and NO2 pollution in Ulaanbaatar, Mongolia, Environmental Research 124: 1-6.

Japan Environmental Agency (2000) Manual for regulation of total emission of nitrogen oxides, Environmental Research and Control Center, Japan.

Kodama, Y., Arashidani, K., Tokui, N., Kawamoto, T., Matsuno, K., Kunugita, N., and Minakawa, N. (2002) Environmental NO_2 concentration and exposure in daily life along main roads in Tokyo, Environmental Research 89: 236-244.

Lee, J.-H., Wu, C.-F., Hoek, G., de Hoogh, K., Beelen, R., Brunekreef, B., and Chan, C.-C. (2014) Land use regression models for estimating individual NOx and NO_2 exposures in a metropolis with a high density of traffic roads and population, Science of the Total Environment 472: 1163-1171.

Marrero, T.R., and Mason, E.A. (1972) Gaseous diffusion coefficients, Journal of Physical Chemistry Reference

Data 1: 3-118.
Mason, E.A., and Malinauskas, A.P. (1983) Gas transport in porous media: The dusty-gas model, Elsevier.
Minakawa, N., Takahashi, K., Nagamune, Y., and Sasaki, J. (2000a) Quality assurance of samplers for suspended particulate matter and their application to field analysis, Bunseki Kagaku 49: 619-624 (in Japanese).
Minakawa, N., Takahashi, K., Nagamune, Y., Koide, N., and Seo, K. (2000b) Quality assurance of automatic nitrogen oxide analyzers and their application to field analysis, Bunseki Kagaku 49: 625 – 630 (in Japanese).
Minoura, H., and Ito, A. (2010) Observation of the primary NO_2 and NO oxidation near the trunk road in Tokyo, Atmospheric Environment 44: 23-29.
Naser, T.M., Kanda, I., Ohara, T., Sakamoto, K., Kobayashi, S., Nitta, H., and Nataami, T. (2009) Analysis of traffic-related NOx and EC concentrations at various distances from major roads in Japan, Atmospheric Environment 43: 2379-2390.
Roorda-Knape, M.C., Janssen, N.A.H., De Hartog, J.J., Van Vliet, P.H.N., Harssema, H., and Brunekreef, B. (1998) Air pollution from traffic in city districts near major motorways, Atmospheric Environment 32: 1921-1930.
van Roosbroeck, S., Wichmann, J., Janssen, N.A.H., Hoek, G., van Wijnen, J.H., Lebret, E., and Brunekreef, B. (2006) Long-term personal exposure to traffic-related air pollution among school children, a validation study, Science of the Total Environment 368: 565-573.
Tiitta, P., Raunemaa, T., Tissari, J., Yli-Tuomi, T., Leskinen, A., Kukkonen, J., Harkonen, J., and Karppinen, A. (2002) Measurements and modeling of $PM_{2.5}$ concentrations near a major road in Kuopio, Finland, Atmospheric Environment 36: 4057-4068.
Uchiyama, S., Aoyagi, S., and Ando, M. (2004) Evaluation of a diffusive sampler for measurement of carbonyl compounds in air, Atmospheric Environment 38: 6319-6326.
US-EPA (last accessed 2015.3.30): MOBILE model (on-road vehicles), Environmental Protection Agency of the United States, <http://www.epa.gov/otaq/mobile.htm>
Wakamatsu, S., Morikawa, T., and Ito, A. (2013) Air Pollution Trends in Japan between 1970 and 2012 and Impact of Urban Air Pollution Countermeasures, Asian Journal of Atmospheric Environment 7: 177-190.
Zhu, Y., Hinds, W.C., Kim, S., Shen, S., and Sioutas, C. (2002) Study of ultrafine particles near a major highway with heavy-duty diesel traffic, Atmospheric Environment 36: 4323-4335.

メキシコシティー中心部道路沿道におけるパッシブサンプラーを用いた二酸化窒素の測定とガウス型プルームパフモデルによる数値予測

神田　勲*・篠原　直秀**・フェリペ　アンヘレス　ガルシア***・若松　伸司****

*愛媛大学農学部生物環境保全学，**産業総合技術研究所，***メキシコ国立環境気候変動局，****愛媛大学農学部生物環境保全学（責任著者）

摘要

メキシコ市中心部の交通量の多い道路近傍における大気環境を評価するために，パッシブサンプラーを道路端から 150 m までの様々な位置に設置して二酸化窒素の濃度を測定した。この測定は，2011 年 11 月に一度，Eje Central 横の Plaza Vizcainas において 24 時間実施された．得られた濃度は，道路端から 2 m および 150 m の地点において，それぞれ約 50 ppbv と 30 ppbv であった．これらの値は，類似の環境における他地点の測定結果と大きく異なるものではなかった．また，観測を実施した期間に対し，ガウス型プルームパフモデルを適用して二酸化窒素の濃度を計算した．窒素酸化物の排出速度は，2003 年の交通量調査，全国排出量インベントリ，および，観測地点における交通量調査を基に推計した．モデル計算による濃度レベルは観測値に近かったが，道路端からの減衰が観測結果よりも大幅に緩やかであった．